



Scanning Imaging Absorption Spectrometer for Atmospheric Chartography carbon monoxide total columns: Statistical evaluation and comparison with chemistry transport model results

A. T. J. de Laat,^{1,2} A. M. S. Gloudemans,¹ I. Aben,¹ M. Krol,^{1,3} J. F. Meirink,⁴
G. R. van der Werf,⁵ and H. Schrijver¹

Received 15 November 2006; revised 7 March 2007; accepted 29 March 2007; published 28 June 2007.

[1] This paper presents a detailed statistical analysis of one year (September 2003 to August 2004) of global Scanning Imaging Absorption Spectrometer for Atmospheric Chartography (SCIAMACHY) carbon monoxide (CO) total column retrievals from the Iterative Maximum Likelihood Method (IMLM) algorithm, version 6.3. SCIAMACHY provides the first solar reflectance measurements of CO and is uniquely sensitive down to the boundary layer. SCIAMACHY measurements and chemistry transport model (CTM) results are compared and jointly evaluated. Significant improvements in agreement occur, especially close to biomass burning emission regions, when the new Global Fire Emissions Database version 2 (GFEDv2) is used with the CTM. Globally, the seasonal variation of the model is very similar to that of the SCIAMACHY measurements. For certain locations, significant differences were found, which are likely related to modeling errors due to CO emission uncertainties. Statistical analysis shows that differences between single SCIAMACHY CO total column measurements and corresponding model results are primarily explained by random instrument noise errors. This strongly suggests that the random instrument noise errors are a good diagnostic for the precision of the measurements. The analysis also indicates that noise in single SCIAMACHY CO measurements is generally greater than actual variations in total columns. It is thus required to average SCIAMACHY data over larger temporal and spatial scales to obtain valuable information. Analyses of monthly averaged SCIAMACHY measurements over $3^{\circ} \times 2^{\circ}$ geographical regions indicates that they are of sufficient accuracy to reveal valuable information about spatial and temporal variations in CO columns and provide an important tool for model validation. A large spatial and temporal variation in instrument noise errors exists which shows a close correspondence with the spatial distribution of surface albedo and cloud cover. This large spatial variability is important for the use of monthly and annual mean SCIAMACHY CO total column measurements. The smallest instrument noise errors of monthly mean $3^{\circ} \times 2^{\circ}$ SCIAMACHY CO total columns measurements are 0.01×10^{18} molecules/cm² for high surface albedo areas over the Sahara. Errors in SCIAMACHY CO total column retrievals due to errors other than instrument noise, like cloud cover, calibration, retrieval uncertainties and averaging kernels are estimated to be about $0.05\text{--}0.1 \times 10^{18}$ molecules/cm² in total. The bias found between model and observations is around $0.05\text{--}0.1 \times 10^{18}$ molecules/cm² (or about 5%) which also includes model errors. This thus provides a best estimate of the currently achievable measurement accuracy for SCIAMACHY CO monthly mean averages.

Citation: de Laat, A. T. J., A. M. S. Gloudemans, I. Aben, M. Krol, J. F. Meirink, G. R. van der Werf, and H. Schrijver (2007), Scanning Imaging Absorption Spectrometer for Atmospheric Chartography carbon monoxide total columns: Statistical evaluation and comparison with chemistry transport model results, *J. Geophys. Res.*, 112, D12310, doi:10.1029/2006JD008256.

¹Netherlands Institute for Space Research, Utrecht, Netherlands.

²Now at Royal Dutch Meteorological Institute, de Bilt, Netherlands.

³Also at Meteorology and Air Quality Group, Wageningen University, Wageningen, Netherlands.

⁴Institute for Marine and Atmospheric Research, Utrecht University, Utrecht, Netherlands.

⁵Faculty of Earth and Life Sciences, Free University, Amsterdam, Netherlands.

1. Introduction

[2] Carbon monoxide (CO) is an important trace gas in tropospheric photochemical processes. CO is removed from the troposphere mainly by reaction with the OH radical which is the major “cleansing” agent of the troposphere [Lelieveld *et al.*, 2004] and the reaction between CO and OH controls the tropospheric OH amount. Furthermore, CO

can lead to tropospheric O₃ production in the presence of nitrogen oxides.

[3] The origins of tropospheric CO are qualitatively well understood [Galanter et al., 2000; Granier et al., 2000; Holloway et al., 2000] and are about evenly distributed between CO from surface emissions, mainly from incomplete combustion in burning processes, and CO from photochemical oxidation of hydrocarbons. About half the surface emissions originate from biomass burning, one third is anthropogenic (fossil fuels) with the remainder originating from various other sources. Biomass burning emissions exhibit strong seasonal and interannual variability [Yurganov, 2000; Wotawa et al., 2001; Langenfelds et al., 2002; Novelli et al., 2003; Yurganov et al., 2005; van der Werf et al., 2006]. Current estimates of CO from oxidation of hydrocarbons show that about 50–60% of CO originates from methane (CH₄) oxidation [Pétron et al., 2002] while about 20% originates from isoprene oxidation and 5–10% from oxidation of terpenes [Granier et al., 2000; Shindell et al., 2006]. Although it is well established which sources contribute to tropospheric CO, the absolute magnitude of individual sources and their seasonality, especially biomass burning emissions, are still uncertain.

[4] Spaceborne measurements from the Measurement of Pollution in the Troposphere (MOPITT) remote sensing instrument, which has been operating from March 2000 onward, have significantly improved knowledge about tropospheric CO variability and its sources. Using mid-infrared channels in the 4.7 micron fundamental CO band, MOPITT has been providing global measurements of tropospheric CO at several tropospheric altitude levels [Deeter et al., 2003, 2004a; Rodgers and Connor, 2003]. MOPITT measurements of CO have been extensively validated [Barret et al., 2003; Heald et al., 2003; Deeter et al., 2004b; Emmons et al., 2004; Crawford et al., 2004] and have been used to study CO variability primarily in the free troposphere [Lamarque et al., 2003; Edwards et al., 2004; Bremer et al., 2004; Lee et al., 2004; Yurganov et al., 2005; Velasco et al., 2005; Edwards et al., 2006] but also for improving CO budgets and emissions [Pfister et al., 2004; Yudin et al., 2004; Arellano et al., 2006].

[5] More recently, first results from the Atmospheric Infrared Sounder (AIRS), which also uses the 4.7 micron CO band and thus has a similar sensitivity to mid-tropospheric CO as MOPITT, have been published, showing great potential for measuring day-to-day mid-tropospheric CO variability [McMillan et al., 2005].

[6] Both the AIRS and MOPITT instruments are not very sensitive to the lower troposphere. The Scanning Imaging Absorption Spectrometer for Atmospheric Cartography (SCIAMACHY) instrument onboard of the Envisat satellite provides the first solar reflectance satellite measurements of CO. Its measurements are close to uniformly sensitive to the entire troposphere down to the Earth's surface [Buchwitz et al., 2005], and deliver unique measurements of total CO columns that are also sensitive to near-surface or boundary layer CO variations, thus complementing the MOPITT and AIRS measurements.

[7] Validation of the near-infrared SCIAMACHY CO total columns with other measurements is complicated [de Laat et al., 2006; Dils et al., 2006]. Comparison with MOPITT is hampered by different measurement sensitivi-

ties of SCIAMACHY and MOPITT for CO at different heights. Ground-based Fourier transform infrared (FTIR) measurements provide high-quality total column measurements but have limited spatial coverage and are located at low surface albedo (<0.2) and/or cloudy regions locations where the SCIAMACHY CO total column measurements are of lower quality [Dils et al., 2006], even for monthly means. Moreover, some of the measurement sites are located on top of mountains which complicate the comparison with satellite measurements because of different footprints [Sussmann and Buchwitz, 2005; Dils et al., 2006]. Furthermore, single SCIAMACHY CO total column measurements (i.e., footprint of 120 × 30 km, or 1–2° × 0.25° longitude-latitude between 60°S to 60°N) are difficult to validate because of their large instrument noise errors. Only when averaging multiple measurements (e.g., monthly means) are the SCIAMACHY CO total columns errors sufficiently small for the measurements to contain useful information on CO [de Laat et al., 2006; Gloudemans et al., 2006]. This is an additional complication for the comparison with ground-based FTIR measurements because often not enough true collocations with cloud free SCIAMACHY measurements are available to obtain monthly mean SCIAMACHY CO total column measurements that have sufficiently small errors for a useful comparison [Dils et al., 2006].

[8] The currently available studies that evaluate SCIAMACHY CO column measurements have been predominantly qualitative by (visually) correlating coherent spatial patterns of SCIAMACHY with MOPITT CO total column measurements or Moderate Resolution Imaging Spectroradiometer (MODIS) fire count maps [Buchwitz et al., 2004, 2005, 2006; Frankenberg et al., 2005].

[9] de Laat et al. [2006] took a different approach by intercomparing CTM simulations and SCIAMACHY measurements to gain insight into both model predictions and instrument errors. Although a CTM model simulation by no means can be considered an absolute truth, it uses actual meteorological input fields and realistic global distributions of CO sources and sinks in its simulation so that seasonal variations in modeled CO should be realistic. Furthermore, model results have been validated against independent measurements like surface-based observations. Finally, model results are available for every single SCIAMACHY measurement, enabling an evaluation of all available data. This allows for a quantification of model-measurement comparison as a function of many relevant parameters. In addition, SCIAMACHY measurements need to be averaged to obtain high enough precision to be of any use. Such temporal and spatial average can be easily represented in the model. The CTM simulation thus provides a very useful tool for intercomparison with SCIAMACHY measurements averaged over large spatial and temporal scales.

[10] de Laat et al. [2006] presented a comparison between modeled and measured seasonal variations in total CO columns and found a good agreement for SCIAMACHY CO total column measurements with small noise errors. The evaluation of SCIAMACHY CO total column measurements by de Laat et al. [2006] was limited to a few locations and served only as a first exploration of this method. This paper continues on this method presenting (1) a detailed and quantitative global analysis of the relation

between surface albedo, cloud cover and measurement errors, (2) comparisons of measured and modeled seasonal cycles with improved biomass burning model emissions from the Global Fire Emission Database version 2 (GFEDv2), (3) global spatial distribution of differences between measured and modeled CO total columns in relation to measurement errors, and (4) statistical analysis of the differences between measured and modeled CO total columns in relation to measurement errors and a statistical analysis of the probability distribution of both model results and measurements with the aim to identify biases.

[11] This paper is organized as follows: Section 2 describes the retrieval algorithm, related calibration issues and error sources in the retrieval. Section 3 describes the TM4 model and a validation with ground based CO measurements. Section 4 presents a detailed statistical evaluation of SCIAMACHY CO total column measurements using TM4 model results. Section 5 ends the paper with conclusions.

2. SCIAMACHY CO Total Columns

2.1. CO Retrievals

[12] The CO total columns are retrieved from spectra measured by SCIAMACHY between 2324.5–2337.9 nm. The retrieval results presented here are derived with the Iterative Maximum Likelihood Method (IMLM) [Gloudemans *et al.*, 2005], which retrieves columns of CO, CH₄ and H₂O simultaneously, as well as surface albedo. In this paper results from the IMLM version v6.3 are used (similar to Gloudemans *et al.* [2006] and de Laat *et al.* [2006]), which uses temperature and humidity profiles based on European Centre for Medium-Range Weather Forecasts (ECMWF) analyses corresponding to the time and location of each SCIAMACHY measurement. Furthermore, the retrieval algorithm uses one a priori CO profile which is scaled as a whole to obtain a good fit to the SCIAMACHY spectrum.

[13] The near-infrared retrievals have proven to be complex because of many instrument/calibration issues described by Gloudemans *et al.* [2005]. The most important ones are the continuous growth of an ice layer on the detectors and the increasing number of dead detector pixels due to radiation damage [Kleipool *et al.*, 2007]. Effects of these instrumental issues have been reduced by applying dedicated in-flight decontamination procedures and additional in-flight calibration measurements, as well as improvements to the calibration [Lichtenberg *et al.*, 2006]. The random instrument noise error is calculated using an instrument model which includes real in-orbit measurements and preflight measurements. The random instrument noise error includes photoelectron shot noise, Johnson noise and detector read-out noise, and also accounts for the integration time of the real in-orbit measurements. Thus the instrument noise error of a single SCIAMACHY measurement is inversely proportional to the number of photons measured, i.e., the measured signal, which is in turn a function of the scene albedo.

[14] The broadening of the slit function due to the growth of the ice layer on SCIAMACHY's channel 8 detector is compensated for by applying an empirical correction which is based on calibrating the retrieved CH₄ total columns from the same retrieval window to CH₄ total columns from a

CTM model simulation. The sensitivity of retrieved CO total columns to this correction has been tested by using CH₄ columns from two different model simulations over two geographical areas: the Sahara and the Australian desert. The average difference in CH₄ columns between these model simulations is between 1 and 2% over both regions. Differences in monthly mean retrieved CO total columns between the four different ice layer corrections are found to be smaller than 2%.

[15] Another source of uncertainty are aerosols, which affect the light path along the line of sight. Tests using desert dust, biomass, industrial, or oceanic aerosols for a large range of solar zenith angles, surface albedos, and aerosol optical depths show that the effect of neglecting aerosols in the retrieval code on the retrieved CO total columns is less than 5%, much smaller than typical real CO total column variations of 10–100% of the annual mean CO total column value. However, measurement biases introduced by aerosols may become important in cases where the random noise error in SCIAMACHY CO total columns is reduced by averaging multiple measurements in, for example, monthly/annual means or area aggregated means.

[16] An example of SCIAMACHY annual mean CO total column measurements for the period September 2003 to August 2004 on a 1° × 1° horizontal resolution is shown in Figure 1. Annual mean CO cannot be accurately determined over oceans because of the very low surface reflectance of oceans at near-infrared wavelengths. High CO columns are measured at middle and high northern latitudes, Southeast Asia, equatorial South America and Africa. Small CO columns occur over the southern parts of South America, Africa and Australia. Mountain ranges can also be discerned (Rocky Mountains, Himalaya, and Andes). The global annual mean distribution of SCIAMACHY CO total columns is qualitatively in good agreement with MOPITT observations (compare for example with Edwards *et al.* [2004]).

2.2. Weighted Means and the Impact of Selection Criteria

[17] The random instrument noise related error of a single SCIAMACHY CO total column measurement is large, typically 10–100% or larger, and is related to the signal-to-noise ratio of the spectral measurements. The latter is determined by variations in surface albedo, solar zenith angle and, to a lesser extent, the ice layer thickness on the channel 8 detector. Single column measurement errors are typically larger than the variability of actual CO total columns. Therefore monthly and annual mean values aggregated at a 3° × 2° horizontal grid are evaluated, as by de Laat *et al.* [2006] and Gloudemans *et al.* [2006]. Single measurements have variable errors, which are taken into account when calculating averages, and for which the weighted averaging procedure as in the work by de Laat *et al.* [2006] is used. In this procedure, the weight of each measurement is taken inversely proportional to the square of the measurement error. Measurements with small errors thus have a larger weight.

[18] The analysis in this paper is restricted to the latitude range of 60°S to 60°N. Poleward of 60° latitude surface albedos are generally below 0.1 and frequent cloud cover

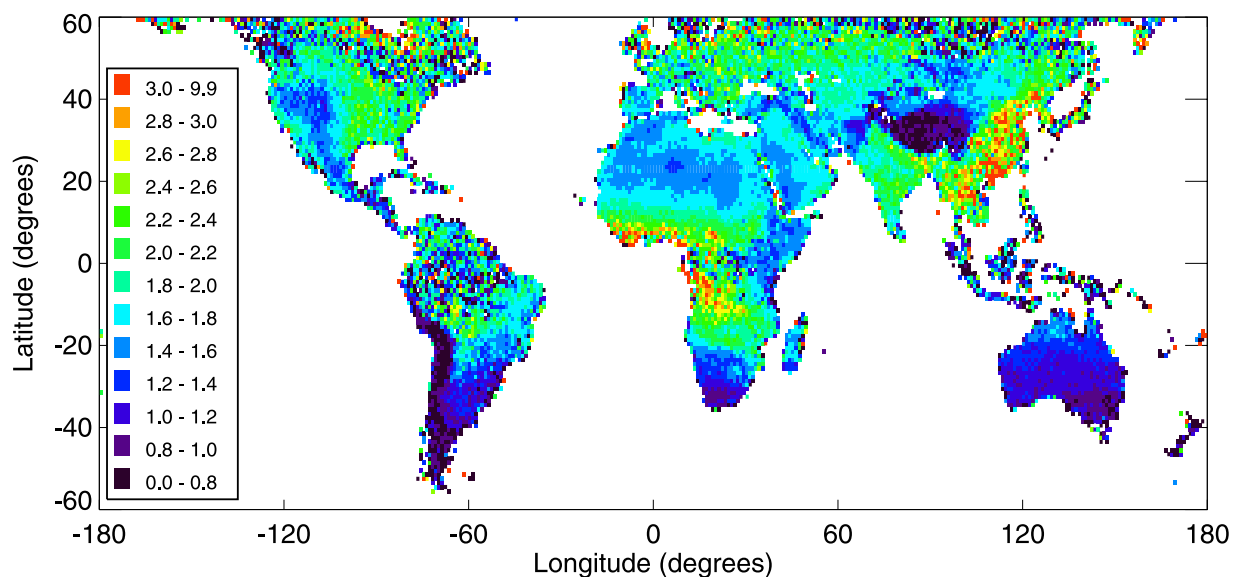


Figure 1. Weighted annual mean Scanning Imaging Absorption Spectrometer for Atmospheric Chartography (SCIAMACHY) CO total columns on $1^\circ \times 1^\circ$ horizontal resolution for September 2003 to August 2004 for land pixels and cloud cover <0.2 only. CO total columns are in 10^{18} molecules/cm². The weighting has been done according to *de Laat et al.* [2006].

occurs. Both effects reduce the number of useful SCIAMACHY measurements significantly. For many high latitudes no measurements can be obtained during winter months because of low solar zenith angle and high cloud cover. The low solar zenith angle also leads to a smaller signal-to-noise. Note that, for clouded regions, averaging all available measurements over one year not always represents a true yearly average. At near-infrared wavelengths the brightest surfaces are dry deserts, not clouds, but the near-infrared albedo of clouds is still higher than that of vegetation (J. M. Krijger, personal communication, 2006).

[19] To ensure that measurements correspond to total CO columns down to Earth's surface all ground pixels with more than 20% cloud cover are excluded. The cloud cover is determined from the number of cloud-free measurements (7×30 km) within one SCIAMACHY ground pixel using the SCIAMACHY polarization measurement device (PMD) Identification of Clouds and Ice (SPICI) algorithm [Krijger et al., 2005]. The SPICI algorithm is based on broadband spectral measurements and can only separate between non-clouded and (partly) clouded observations. The derived cloud cover is therefore an upper estimate of the actual cloud cover because PMD observations labeled "clouded" can also be partially clouded. The significance of differences in cloud cover thresholds has also been tested. A more stringent cloud cover threshold results in fewer "cloud-free" measurements. Different cloud cover thresholds of 0, 10 or 20% cloud cover result in differences in monthly mean CO total columns of up to $\pm 30\%$. However, most of these differences are not significant in relation to their large random instrument noise error (at the 95% confidence level). Note that the largest differences due to different cloud cover thresholds occur for locations where random

instrument noise errors are large because of low surface reflectances.

3. Validation of TM4 Model With Ground-Based Measurements

3.1. TM4 Model and Emissions

[20] The global chemistry-transport model TM4 [Meirink et al., 2006] used for this study is a follow-up of TM3 [Dentener et al., 2003, and references therein]. Differences between TM3 and TM4 are described by Meirink et al. [2006]. Meteorological ECMWF analysis input fields used in TM4 are preprocessed as described by Bregman et al. [2003].

[21] CO emissions are as described by Dentener et al. [2003]. This means that natural emissions are as in the work by Houweling et al. [1998] and anthropogenic emissions are based on van Aardenne et al. [2001], extrapolated to the year 2000 using the same method as described by Dentener et al. [2003]. Table 1 gives the resulting annual total CO emissions. For fossil fuel emissions at latitudes $>45^\circ$ a seasonal variation was added, with up to 15% (9%) higher (lower) emissions in winter (summer). For biomass burning emissions the seasonality from Hao and Liu [1994] was applied. However, most results shown in this paper do not rely on climatological but on biomass burning emission estimates for 2003 and 2004 from the GFEDv2 database [van der Werf et al., 2006], which was also used by Gloude-mans et al. [2006]. The GFEDv2 CO emissions are based on satellite measurements of fires and burned area (MODIS). See van der Werf et al. [2006] for a detailed description of which satellite data were used for which period. Biomass burning emissions typically contribute about one third to the total CO emissions [Granier et al., 1996; Galanter et al., 2000; Pétron et al., 2004]. The large

Table 1. Global Annual Total CO Emissions^a

	VA2001			GFED v2		
	Global	Africa	South America	Global	Africa	South America
Fossil fuels	331					
Biofuels	194					
Biomass burning	554	192	115	397 (2003), 404 (2004), 432 (1997–2004)	160 (2003), 164 (2004), 174 (1997–2004)	62 (2003), 99 (2004), 66 (1997–2004)
Natural	115					
Total	1194					

^aUnit is Tg CO yr⁻¹. VA2001 refers to *van Aardenne et al.* [2001]. GFEDv2 are available for the period 1997–2004.

differences in biomass burning emission estimates have a significant impact on modeled CO total columns and explain many differences between model results and measurements reported by *de Laat et al.* [2006], as will be shown in section 4.1.

[22] The CO total column averaging kernels, similar to *Buchwitz et al.* [2004], are close to 1 up to ~200 hPa indicating that CO variations in the lower troposphere can also be measured by SCIAMACHY. One year of individual modeled CO columns with and without applying the total column averaging kernels have been calculated. Differences were found to be smaller than ±2% while on average close to zero. Therefore the CTM modeled CO total columns are used here without applying total column averaging kernels.

[23] For every single SCIAMACHY CO total column measurement the temporally and spatially collocated TM4 modeled CO total column was obtained. Monthly and annual averages of the model are thus based on collocated measurements.

3.2. Validation of TM4 Modeled CO With Ground-Based Measurements

[24] In the work by *de Laat et al.* [2006] model results have been compared to Global Monitoring Division (GMD, previously CMDL) surface CO measurements [*Novelli et al.*, 2003] for the period 2003–2004. It has been shown that TM4 modeled annual mean and seasonal and short-time variability are consistent with GMD measurements. Figure 2 shows a different representation of those results using a Taylor diagram [*Taylor*, 2001]. A Taylor diagram is a graphical visualization of the correlation, variability and root-mean-square differences of two series (see Figure 2 caption). The curved lines in the diagram indicate the skill of the model result, i.e., how well the GMD measurements are reproduced by the model, which is defined as:

$$S = \frac{(1 + R)^2}{(\sigma_f + 1/\sigma_f)^2}$$

[25] With S the skill level (varying between 0 and 1), R is the correlation coefficient and σ_f the ratio of modeled and measured standard deviation. In cases where modeled and measured standard deviations are comparable and the correlations are high (R close to 1) the skill level will be close to 1 and modeled CO is very similar to measured CO. A skill level 0 indicates no resemblance between of measured and modeled CO. Note that the skill level is not sensitive for a systematic bias in the model or the measurements.

[26] Figure 2a shows that the locations can be grouped according to a skill level of 0.6. Locations with skill levels >0.6 show a good to excellent correlation (0.6–0.95) with reasonable to good modeled variability. High correlations generally indicate similar seasonal cycles. This group includes remote Northern and Southern Hemisphere locations. Here “remote” means no important emissions sources in the immediate vicinity of the location. Interestingly, model variability is consistently too small at Southern Hemisphere remote locations. However, a model simulation with different emissions yielded the opposite result (systematically too large modeled variability), indicating that even remote locations are sensitive to the accuracy of model emissions because of long-range transport and the long atmospheric residence time of CO.

[27] The second group of locations have skill levels <0.6 and do not contain remote locations. An evaluation of these locations indicates that all of them are close to large emissions sources. There are several possible explanations for the smaller skill levels. Model emissions amounts may be inaccurate, as well as their geographical distribution and seasonality. Furthermore, locations may be affected by local emissions or local circulation patterns. Modeling the latter two processes requires a much finer resolution than current TM4 model resolution. Although it is beyond the scope of this paper to present a detailed analysis of the surface station comparison, it must be mentioned that most of these discrepancies can be understood in terms of the site location and its vicinity to emission sources. In general the agreement for the locations with skill levels <0.6 improves when selecting a nearby model grid cell that can be considered more representative of these locations. It should be noted that *Shindell et al.* [2006] also compared model results with GMD measurements and that considerable biases were found, but they do not apply an interpolation between model grid cells to the actual station location, nor discuss the effect of model resolution in the vicinity of large CO sources. In addition, this study uses the satellite-based GFEDv2 biomass burning emission estimates compared to biomass burning climatologies given by *Shindell et al.* [2006].

[28] Figure 2b shows that the latitudinal variation of the average modeled and measured surface CO concentrations for all locations shown in Figure 2a agree well. The modeled and observed latitudinal gradient are similar: low CO concentrations in the Southern Hemisphere, a tropical increase, and high CO concentrations in the Northern Hemisphere as well as the occasional very high Northern Hemisphere concentrations for locations close to CO sources. However, modeled Northern Hemisphere CO concen-

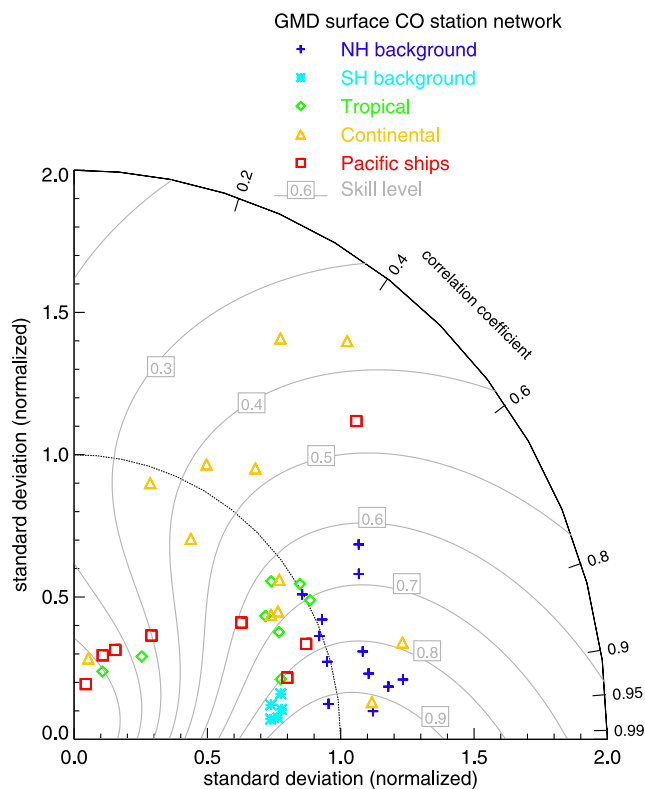


Figure 2a. Taylor diagram of TM4 modeled and Global Monitoring Division (GMD) surface measurements of CO for the period 2003–2004. All available data were used, e.g., no averaging or filtering was applied to the data. The correlation coefficient between the observed and simulated field is given by the cosine of the azimuthal angle, the ratio of the standard deviations of the observed and simulated fields is proportional to the radial distance, and the centered root-mean-square difference between the two fields is proportional to the distance from any point on the diagram to the standard deviation value 1.0 on the x axis. The color coding of the GMD surface stations is based on five groups of locations: Northern and Southern Hemispheric remote locations, tropical locations, continental locations, and Pacific fixed latitude ship tracks. The standard deviation of the model results is scaled by the standard deviation of the measurements at the corresponding GMD station. The grey lines in the diagram indicate a skill level (ranging from 0 to 1). A perfect representation of the measurements by the model would have a correlation of 1 and a scaled standard deviation of 1.

trations are on average 10–20% lower than observed. All models in the work by *Shindell et al.* [2006] also showed an underestimation of CO with respect to GMD measurements in the Northern Hemisphere. Compared to most of these models, the underestimation in the present model simulation is relatively small. This may be due to the different emission inventory used, to the seasonality applied to fossil fuel emissions (relatively more CO emitted in winter when the lifetime is long), or some other difference. Part of the low bias in the Northern Hemisphere may be related to the close vicinity of a number of measurement sites to major emission regions, but probably inaccurate emission estimates or other

model inaccuracies due to chemistry and transport play a role as well.

[29] Figure 2c shows a comparison of individual FTIR measured and TM4 modeled CO total columns at Lauder, New Zealand and Izaña, Tenerife, Canary Islands. Izaña is located at an altitude of approximately 2 km and the CO total columns measurements there represent free tropospheric CO. Modeled CO columns above 2.4 km were used in Figure 2c for the comparison at Izaña. At Lauder, the model results also indicate that about 90% of the CO total column and 90% of the column variability is located above 1 km altitude. A good agreement between measured and modeled CO total columns is found for both locations. Note that by removing the high modeled CO total columns at Lauder in the beginning of 2003 (5 occurrences) the time correlation becomes significantly higher at 0.75. This comparison indicates that modeled free tropospheric CO total columns agree with the independent FTIR observations.

[30] The agreement between modeled and measured surface and free tropospheric spatial and temporal CO variations shows that transport and chemistry of CO as well as the geographical distribution of CO sources are realistically modeled. The quality of the TM4 CO is therefore considered sufficient for validation and evaluation purposes. As will be shown, the comparison with model results gives interesting information about the quality of the SCIAMACHY total CO columns. On the other hand, model emissions estimates clearly leave room for improvement, for which satellite observations may be best suited.

4. SCIAMACHY CO Total Column Results

4.1. Comparison of TM4 and SCIAMACHY Seasonal Cycles for Individual Locations

[31] Figure 3 shows a comparison of seasonal variations of monthly averaged SCIAMACHY CO total columns with the two different model versions described in section 3.1, i.e., the climatological emissions and the GFEDv2 emissions. Several $3^\circ \times 2^\circ$ grid cells for the period September 2003 to August 2004 are shown (see Table 2). These locations are different from those shown by *de Laat et al.* [2006] and represent a range of different situations with regard to the seasonal cycle and instrument noise errors. The same error filter as given by *de Laat et al.* [2006] has been used for the calculation of the monthly means: single SCIAMACHY CO total column measurements with instrument noise errors $>1.5 \times 10^{18}$ molecules cm^{-2} (i.e., on the order of typical CO total column values) are excluded from the calculation of monthly means. Figure 3 highlights different seasonalities, instrument noise errors due to variations in albedo and cloud cover and issues related to model errors and interpretation of results. Table 2 summarizes the statistics of this comparison for the locations in Figure 3.

[32] For locations A to I a significant improvement is found for the comparison of SCIAMACHY measurements with the model results when using GFEDv2 biomass burning emissions. These locations are scattered around the globe and represent very different seasonal cycles. Sporadically, outliers occur like for location B, D, L and O. Most of the outliers (differences with TM4 $> 2\sigma$ instrument noise error) with small CO total columns have monthly means based on only a few measurements, and the

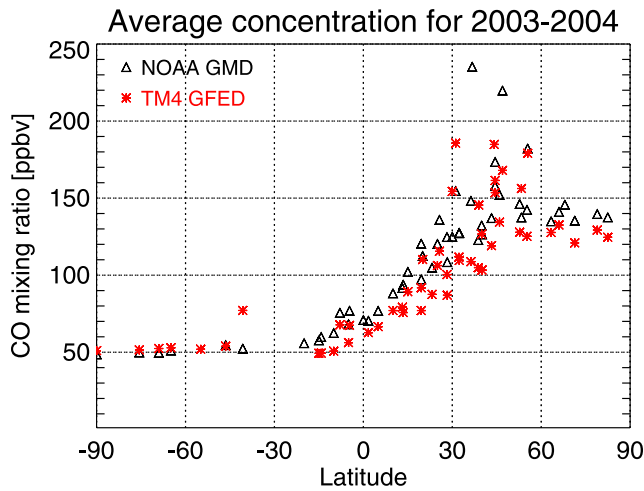


Figure 2b. Latitudinal distribution of average CO surface concentrations for the period 2003–2004 for the GMD measurements (black triangles) and TM4 model results (red asterisks).

error bars in Figure 3 indicate that the monthly means are not very accurate. The small CO total columns are mostly related to clouds and mainly occur at locations with low surface reflectances (<0.1). As explained in section 2.2 we allow for a maximum cloud cover of 20% in the observations. Although in most cases the cloud cover is much lower than this, in the cases where some cloud contamination is present, combined with a low surface reflectance (<0.1), the signal from the cloud contaminated part of the SCIAMACHY ground scene can dominate the total signal of the measurements. Indeed for most of the outliers at least

one of the measurements in the monthly mean shows either a relatively high cloud fraction or low methane values in combination with low surface reflectance. Such a contaminated measurement significantly changes the monthly mean if only a few measurements are averaged. This effect will be significantly less in case of averaging many measurements.

[33] For location D monthly variations in surface albedo and the number of “cloud-free” measurements are printed within Figure 3 to indicate the dependence of monthly mean measurement errors on cloud cover and surface albedo. For example, June has a very large instrument noise error due to a low albedo and just one collocation.

[34] Location G in Iran shows a distinct peak during mid winter in both model results and measurements likely related to wintertime continental accumulation of CO. However, the instrument noise error of the measurements is too large to provide a decisive answer as to which model simulation shows the best agreement. Results from both model simulations fall within the measurement uncertainty.

[35] For location J the instrument noise errors are small but the agreement with the model results is not very good. This location in northern South Africa shows good agreement from December 2003 onward but the peak from September to November 2003 is not reproduced by either of the model simulations. This is a region where an incorrect biomass burning season cycle was identified in the model simulation with climatological biomass burning emissions [de Laat et al., 2006]. For the climatological emissions modeled CO columns are higher between May and August because of the incorrect timing of the biomass burning season. For the model simulation with GFEDv2 biomass burning emissions the agreement is much better throughout the region during boreal summer 2004. During

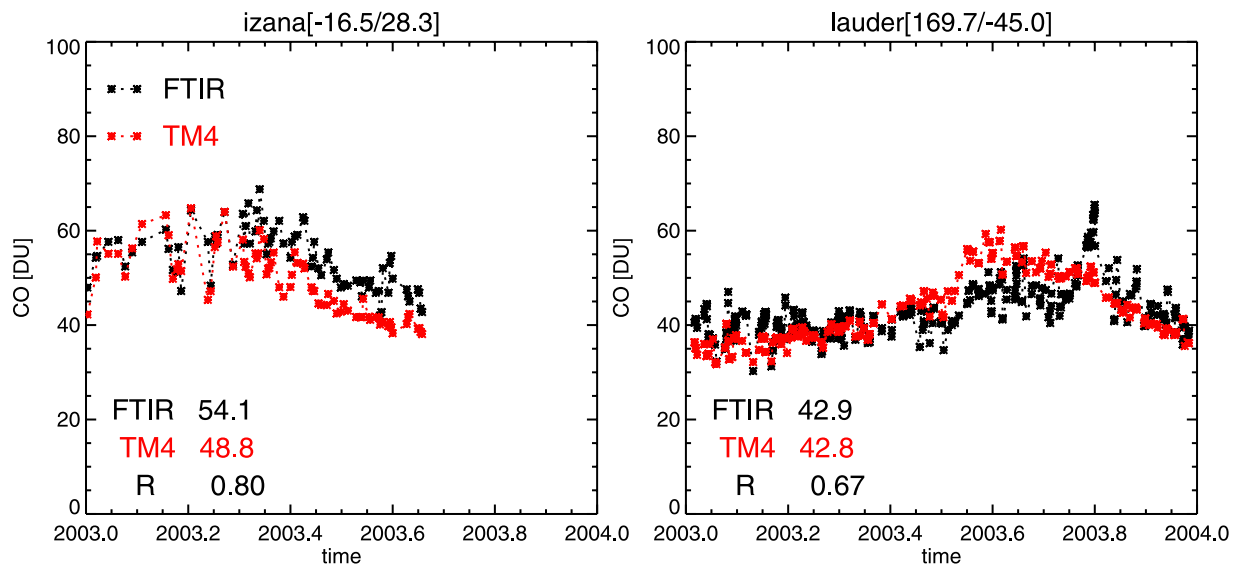


Figure 2c. Fourier transform infrared (FTIR) measurements of CO total columns at Izaña (approximately 2400 m altitude) and Lauder (370 m altitude), New Zealand, for the year 2003 and corresponding modeled TM4 columns. Measurements used here were obtained as part of the Network for the Detection of Atmospheric Composition Change (NDACC) and are publicly available (see <http://www.ndacc.org>). Indicated in Figure 2c are also the average CO total column values for TM4 and the FTIR measurements and their temporal correlation.

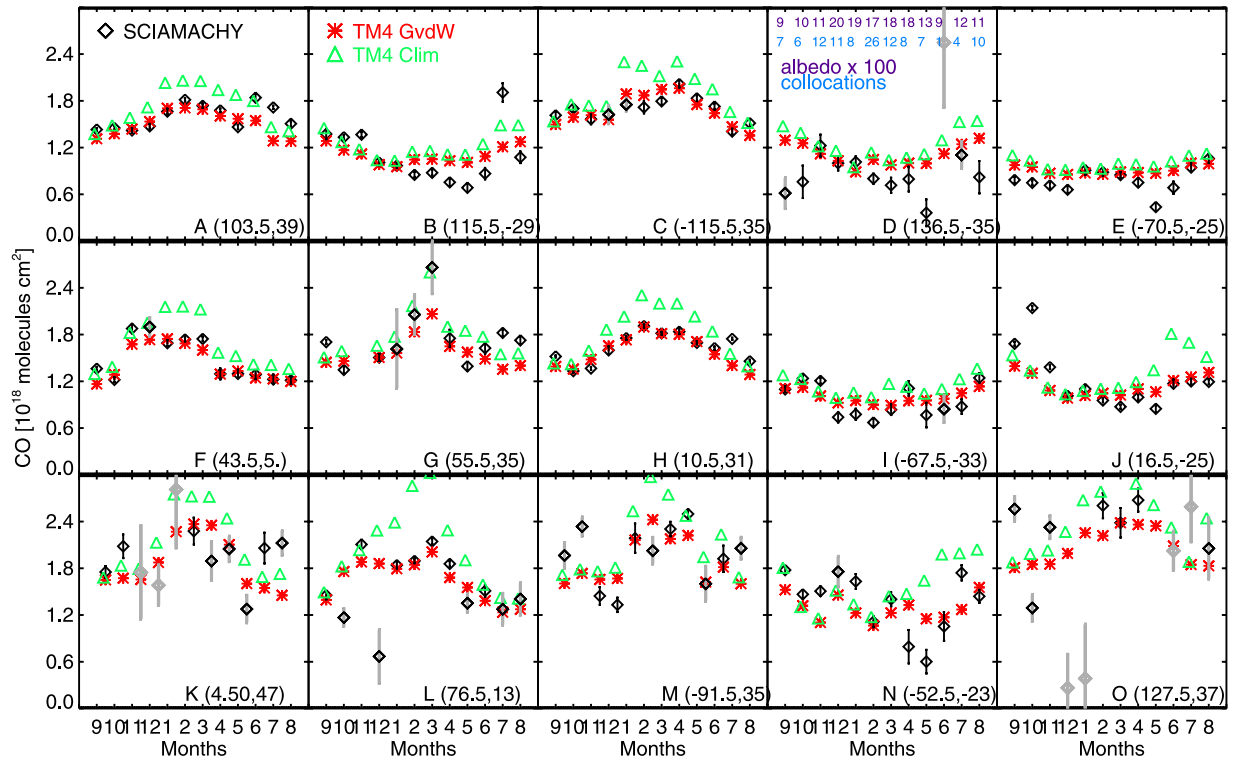


Figure 3. Comparison of seasonal cycles for a selection of locations shown in Figure 6. The period shown is arranged such that the first month (month 9) refers to September 2003; month 1 is January 2004. The error bars of the measurements indicate the 1σ instrument noise error. The grey error bars indicate locations where the monthly mean is based on 5 or less single measurements, and a grey marker indicates that the average monthly surface albedo is below 0.1. For location D the monthly albedos ($\times 100$) and number of collocations used to calculate monthly means are also indicated in the top of the panel. See Table 2 for statistics corresponding to locations A–O.

boreal autumn 2003 (month 9 onward) measured CO total columns are still higher than the modeled values. *Gloude-mans et al.* [2006] reported similar findings. *Van der Werf et al.* [2006], however, note that frequent cloud

cover, the low spatial resolution of their modeling framework, and neglecting emission variations on timescales less than a month may lead to an underestimation of the GFEDv2 emissions in biomass burning regions.

Table 2. Measurement Statistics of the SCIAMACHY-TM4 Comparison for the Locations Presented in Figure 3^a

	Longitude/Latitude	ε	Δ	$ \Delta $	$\sigma(\Delta)$	N	Albedo	Δc	$ \Delta c $	$\sigma(\Delta c)$
A	103.5/39	1.9	6.4	8.9	10.5	7–40 (21)	0.34–0.39 (0.36)	–9.0	14.1	14.1
B	115.5/–29	5.0	–1.1	20.5	27.1	9–39 (23)	0.14–0.29 (0.23)	–13.0	23.3	25.0
C	–115.5/35	3.4	0.6	6.1	6.8	4–31 (16)	0.19–0.27 (0.25)	–13.5	14.2	11.4
D	136.5/–35	19.7	–12.4	39.2	54.1	1–26 \pm 9)	0.10–0.21 (0.15)	–25.7	47.1	54.7
E	–70.5/–25	5.5	–13.6	16.0	15.4	10–26 (17)	0.21–0.27 (0.24)	–24.0	24.0	15.4
F	43.5/5	3.6	3.8	5.7	6.8	4–31 (17)	0.23–0.30 (0.27)	–13.7	15.1	12.0
G	55.5/35	9.6	11.7	15.4	16.2	1–33 (13)	0.12–0.30 (0.24)	–4.6	13.2	14.9
H	10.5/31	1.5	3.2	5.5	7.8	7–45 (26)	0.40–0.49 (0.46)	–12.0	15.7	13.0
I	–67.5/–33	4.6	–18.3	14.0	15.1	3–30 (16)	0.14–0.22 (0.18)	–46.8	49.8	53.7
J	16.5/–25	3.0	5.5	16.7	25.3	11–43 (26)	0.26–0.33 (0.29)	–9.7	27.4	34.1
K	4.5/47	15.1	5.7	18.3	22.0	1–20 \pm 8)	0.08–0.14 (0.10)	–9.1	20.9	24.3
L	76.5/13	6.2	–4.7	14.0	23.2	1–40 (14)	0.16–0.26 (0.22)	–27.5	28.2	28.0
M	–91.5/35	7.0	4.5	13.5	16.4	3–25 (13)	0.08–0.24 (0.14)	–9.3	20.3	22.2
N	–52.5/–23	8.7	–22.4	5.6	26.3	4–29 (17)	0.11–0.16 (0.13)	–16.5	29.8	36.9
O	127.5/37	13.2	–0.6	33.0	45.1	1–17 \pm 8)	0.06–0.13 (0.10)	–16.9	37.4	47.7

^aIndicated are geographical locations (central point of the $3^\circ \times 2^\circ$ longitude-latitude grid), average monthly mean instrument noise error (ε ,%), average monthly mean differences (Δ ,%), The average of the absolute monthly differences ($|\Delta|$,%), standard deviation of the monthly mean differences ($\sigma(\Delta)$,%), range of the number of monthly SCIAMACHY measurements (N) for each grid box (in brackets average monthly number of measurements), surface albedo range (in brackets average monthly surface albedo), average monthly mean differences using the climatological emissions (Δc ,%), the average absolute monthly mean differences using the climatological emissions ($|\Delta c|$,%) and standard deviation value of the monthly mean differences using the climatological emissions ($\sigma(\Delta c)$,%). The geographical locations of the selected grids are shown in Figure 6. All values are expressed as percentage of the annual mean modeled TM4 CO total column.

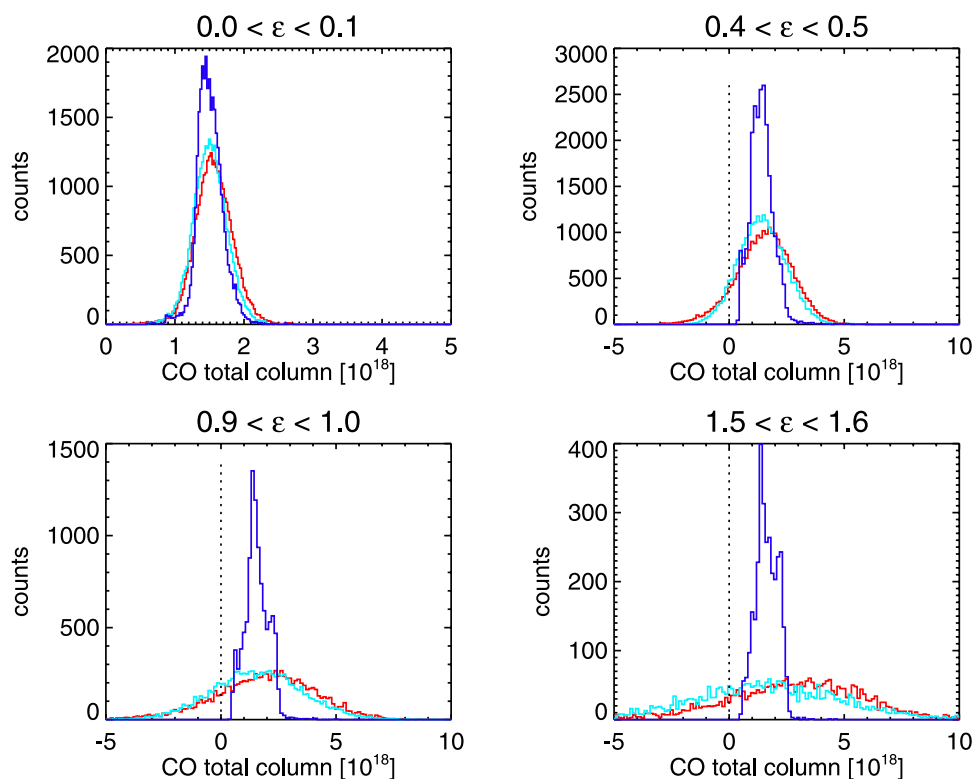


Figure 4. Probability density functions for single SCIAMACHY and corresponding TM4 CO total columns for four different SCIAMACHY instrument noise intervals indicated at the top of each panel in 10^{18} molecules/cm². The red line indicates the SCIAMACHY probability distribution functions (PDF), the dark blue line indicates the TM4 PDF while the light blue line is represents the PDF of TM4 results convoluted with artificial noise (Gaussian) corresponding to the selected measurement noise interval. Note the different x axis range for the top left plot.

[36] For locations K, M, N and O the agreement between model results and measurements is not very good. Location K, M and N are close to emission sources, the surface albedo is small and many measurements are affected by clouds. The vicinity of emission sources is apparent in the large differences between the TM4 CO total columns with climatological emissions and the GFEDv2 emissions. Location O (northeastern China) is remote from emission sources, but the surface albedo is small and many measurements are affected by clouds. Very likely the outliers for December and January are related to clouds (see end of section 2.2) as they are based on 2 and 1 collocations, respectively. Location L (India) is also close to emission sources but the surface albedos are higher. If September and December, months with few collocations, are left out, the agreement is actually good.

[37] In general, the comparison between SCIAMACHY and TM4 CO total columns improves significantly with the GFEDv2 model biomass burning emissions. For nearly all locations the average monthly differences, the average of the absolute monthly differences and standard deviations improve with the GFEDv2 biomass burning emissions compared to the climatological emissions (Table 2). Total CO columns from the simulation with the GFEDv2 biomass burning emissions are generally lower than those from the climatological emissions and more in agreement with the

measurements. Also, the timing of the biomass burning emissions is much improved using the GFEDv2 satellite derived emissions. Therefore the model results including the GFEDv2 emissions are used in the remainder of the paper.

4.2. SCIAMACHY Single-Column Measurements Analysis

[38] In order to test whether the differences between SCIAMACHY CO and the model results with the GFEDv2 emissions shown in Figure 3 are significant or fall within the measurement noise error a more detailed statistical analysis has been performed. A first general test of the quality of SCIAMACHY CO total column measurements is to compare differences between modeled and measured CO total columns in relation to instrument noise errors. *de Laat et al.* [2006] already noted that a large variation in instrument noise errors is present in the measurements primarily because of varying albedos and loss of data due to cloud cover.

[39] Figure 4 compares probability distribution functions (PDF) of measured (red lines) and modeled (dark blue lines) single CO total columns for different instrument noise intervals expressed in terms of equivalent CO total column error. One year (September 2003 to August 2004) of global SCIAMACHY data and spatially and temporally collocated TM4 data is used. The effect of instrument noise errors on

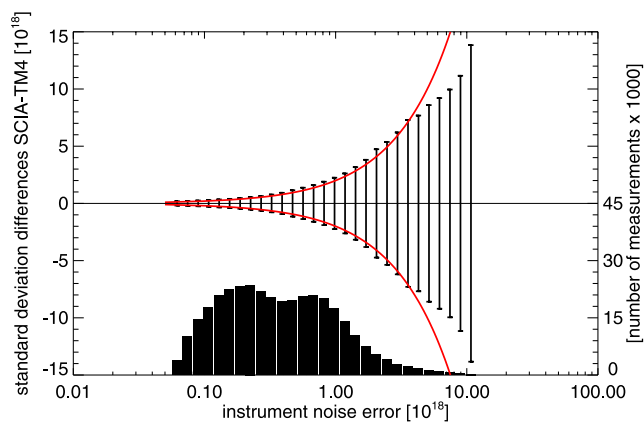


Figure 5a. Probability distribution of the standard deviation of SCIAMACHY-TM4 differences as a function of instrument noise errors based on single SCIAMACHY measurement-TM4 differences as a function of instrument error. The SCIAMACHY-TM4 differences are binned according to their instrument noise error, after which the standard deviation value is calculated for all differences with a certain error interval. The red line indicates the $(2\text{-}\sigma)$ error, whereas black lines indicate the standard deviation of the differences. The black bars at the bottom of the graph indicate the total number of measurements with instrument noise errors for a certain error interval. This graph is based on one year of SCIAMACHY measurements from September 2003 to August 2004 between 60°S and 60°N .

the PDF is clearly visible. For small instrument noise errors (Figure 4, top left) the distributions are very similar, but with increasing errors the measurement distribution becomes wider. The light blue lines show the model distributions when convoluted with artificial noise that corresponds to the instrument noise error. With this convolution the measurement and model results distributions become more similar. Differences are found in the width of the distribution

(Figure 4, top right) and in the mean CO total columns causing shifts in the distributions (Figure 4, bottom right). These differences are caused either by modeling errors and/or biases in the retrieval algorithm.

[40] Figure 5a shows the standard deviation of the differences between single SCIAMACHY measurements of the total CO column and the temporally and spatially collocated modeled CO total columns. By evaluating the SCIAMACHY-TM4 differences the spatial variability of CO is taken into account. For an ideal model simulation, and assuming that the measurement errors are well characterized, the standard deviation of the differences should equal the corresponding instrument noise error. The results are grouped according to the corresponding instrument noise errors. The red line represents the instrument noise error. The standard deviation of the differences between SCIAMACHY measurements and model results follow the instrument noise error level: the larger the noise error, the larger the standard deviation of the differences. Only for very large instrument noise errors ($>5 \times 10^{18}$ molecules/cm²) this relation breaks down. However, it should be noted that only a limited number of measurements have such large instrument noise errors.

[41] Figure 5b shows the average difference between SCIAMACHY and modeled CO total columns per noise error interval. Differences remain close to zero ($<0.08 \times 10^{18}$ molecules/cm²) for instrument noise errors smaller than about 1×10^{18} molecules/cm². For larger instrument noise errors the measurements become on average positively biased compared to the model results. This result provides the motivation for excluding measurements with instrument noise errors $>1.5 \times 10^{18}$ molecules/cm² in the calculation of monthly and annual means that are used in sections 4.1 and 4.3 or Figure 3. This procedure was also followed by *de Laat et al.* [2006] and *Gloudemans et al.* [2006]. Using this procedure removes only about 10% of the measurements with cloud cover $<20\%$; nearly all (99.8%) of the measurements that are removed have an albedo <0.1 , and 80% have an albedo <0.05 .

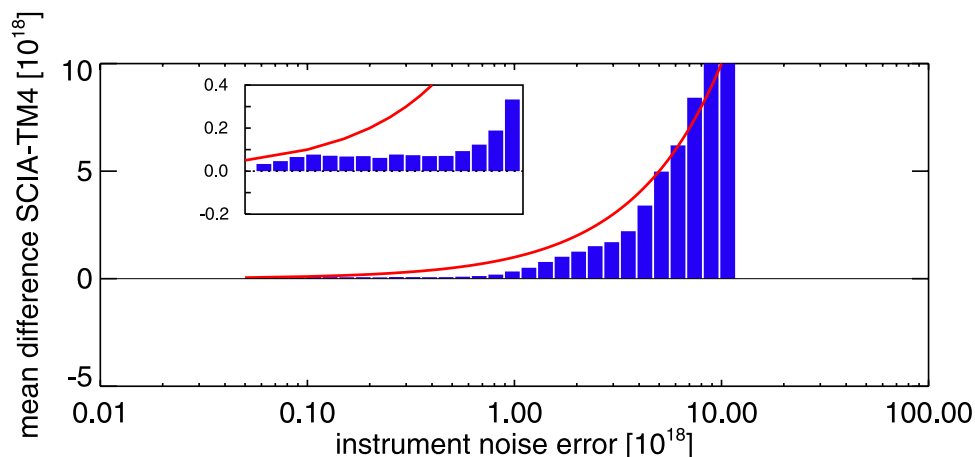


Figure 5b. Average differences (blue) between the SCIAMACHY and TM4 corresponding to Figure 5a. The red line indicates the (σ) error. The insert shows a magnification of the differences for the instrument noise error interval between 0.05×10^{18} and 1×10^{18} molecules/cm².

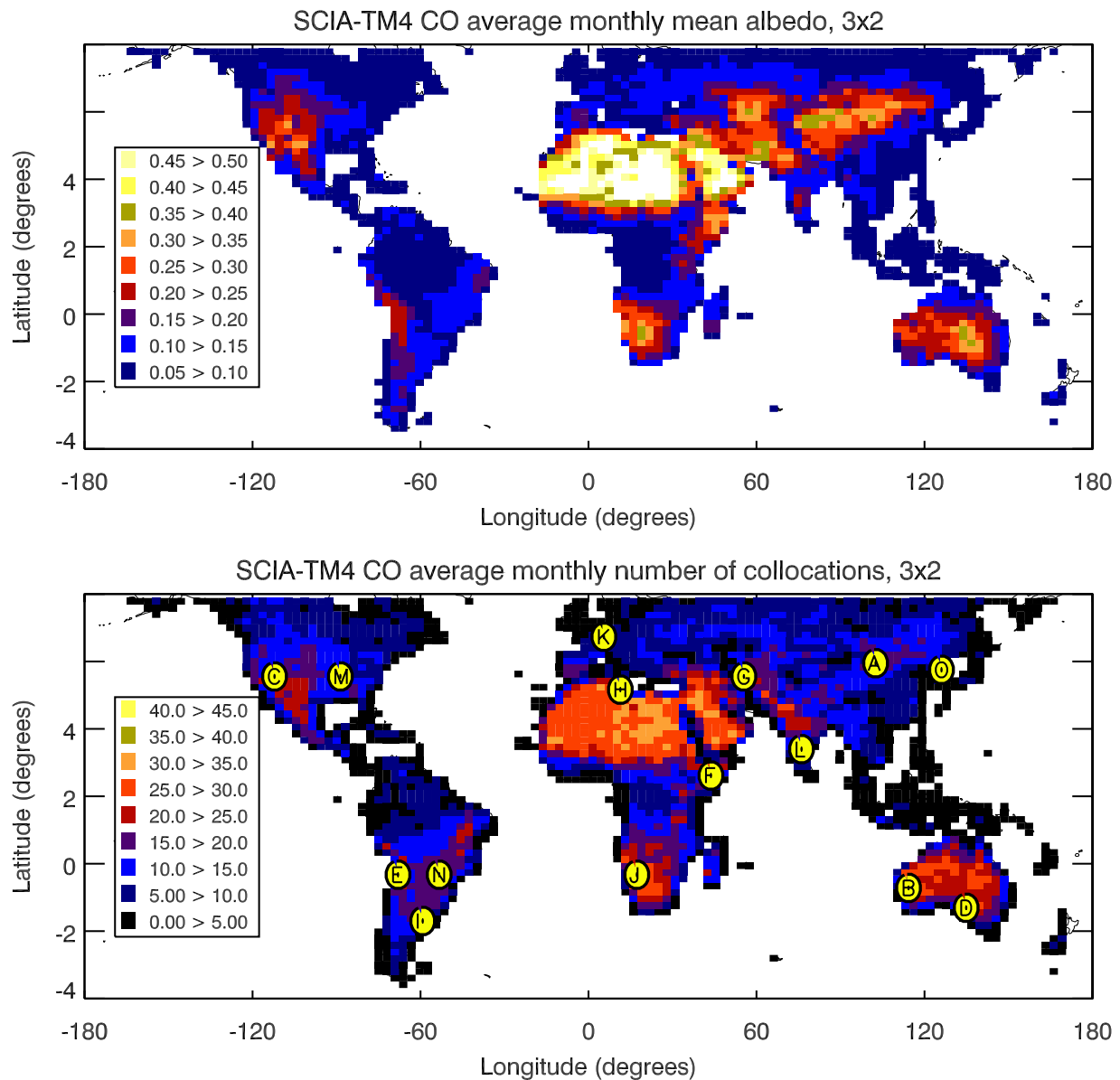


Figure 6. (top) Geographical distributions of the average monthly mean surface albedo, which is a product of the retrieval algorithm, for the period September 2003 to August 2004 for partial land pixels. (bottom) Geographical distribution of average number of measurements per month for the same selection of grids as shown in Figure 6 (top). Indicated are also the locations of the grids shown in Figure 3.

[42] The results presented in this section clearly show the importance of instrument noise errors in the measurements. The instrument noise error is by far the dominant error source and thus provides a good estimate of the precision of a single SCIAMACHY measurement. Section 4.3 will discuss the origins of the large variations in instrument noise errors in more detail, and how they relate to differences between modeled and measured CO total columns.

[43] It should also be noted that because of the large instrument noise errors, the measured columns can become negative, as observed in Figure 4 for instrument noise error levels $>0.2 \cdot 10^{18}$ molecules/cm². Although a negative column may intuitively be considered physically unrealistic, Figure 4 indicates that these negative values should be kept in the analysis, otherwise the Gaussian distribution would

break down, and averaging multiple measurements would lead to positive biases.

4.3. SCIAMACHY Monthly and Annual Means Analysis

[44] As shown in section 2.2, the instrument noise errors for single SCIAMACHY measurements depend on their signal-to-noise ratio. In the region between 60°S and 60°N the signal-to-noise ratio depends mostly on the surface albedo. It is important to understand the spatial variation of both parameters. Figure 6 shows the monthly average albedo and monthly number of cloud free measurements as used for the calculation of monthly mean CO values. The period that is analyzed here runs from September 2003 to August 2004. The total number of measurements averaged

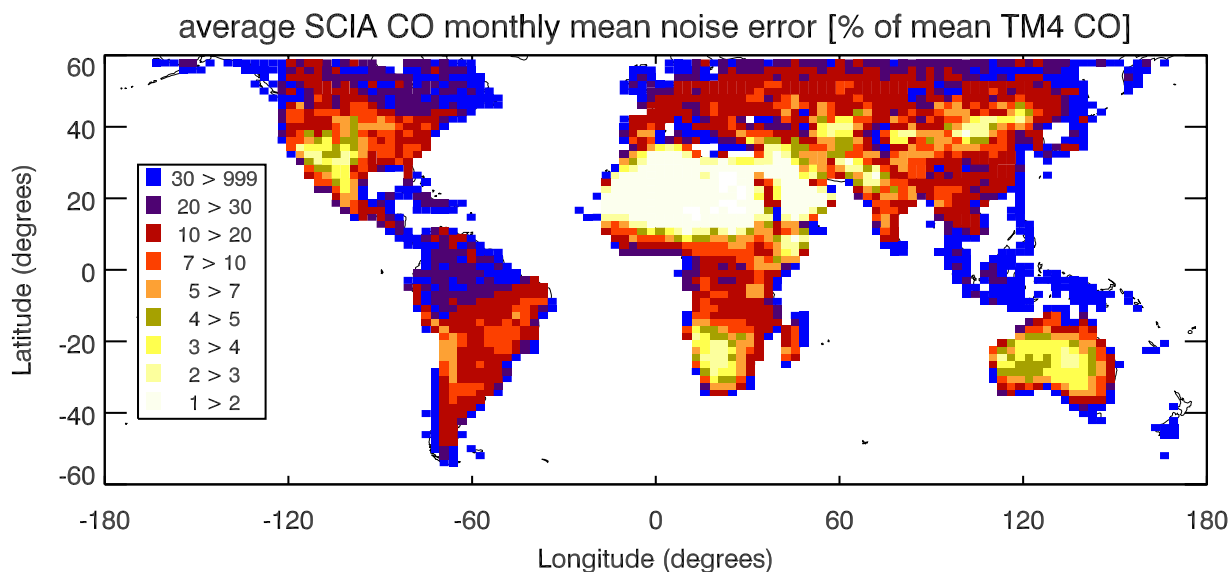


Figure 7. Similar to Figure 6 but for the average SCIAMACHY CO total column monthly mean instrument noise errors for the period September 2003 to August 2004. Noise errors are shown as in 10^{18} molecules/cm².

in a $3^\circ \times 2^\circ$ monthly or annual mean is primarily determined by the cloud cover threshold that is used to select the “cloud-free” SCIAMACHY CO measurements. High surface albedos larger than 0.4 are found over dry deserts and semideserts. Vegetated regions have a low surface albedo, smaller than 0.1. Dry regions also have much more cloud-free scenes than vegetated regions (up to factor of 5–6). Cloud cover and albedo have very similar spatial patterns and thus reinforce each other in their effect on the spatial distribution of monthly and annual mean instrument noise errors.

[45] Figure 7 shows the spatial distribution of the average monthly mean instrument noise error, which is very similar to the spatial distributions of cloud-free pixels and surface albedo. The combined effect of high albedo and low cloud cover over subtropical desert regions results in monthly mean instrument noise errors that are up to 25 times smaller than for example instrument noise errors at high-latitude locations. This large variation in monthly mean noise errors should be considered when using the SCIAMACHY CO measurements. In the work by *de Laat et al.* [2006] annual mean CO total columns from SCIAMACHY and TM4 were compared and instrument noise errors of annual means were presented but it was not investigated in detail how differences between measurements and model results relate to the instrument noise error.

[46] Figure 8 shows the differences between measured and modeled annual mean CO total columns. Differences smaller than 5% of the local annual mean modeled CO total columns are shown as greys. Measured Northern Hemisphere CO is higher than modeled CO (typically 5–20%; up to 50%), with larger measured CO total columns (>25%) over Canada, east Siberia and east Asia, which could be related to the extensive forest fires that occurred in this region in 2003 [*Yurganov et al.*, 2005] and 2004. Measured CO columns are also larger in parts of eastern South America, southern Africa, and northern Australia, which

are all well-known fire regions. Smaller CO can be found in a few equatorial areas, most notably central Africa and Indonesia which are close to large emission sources [e.g., *Bremer et al.*, 2004; *Velazco et al.*, 2005].

[47] Figure 8 (bottom) shows those grid cells for which differences are larger than 5% and larger than the $2\text{-}\sigma$ instrument noise error (95% confidence level). For most locations measured and modeled CO total columns agree within the $2\text{-}\sigma$ error and differences are thus not significant, but a few areas with large differences (>25%) remain: northwestern USA, eastern South America, southern Africa and eastern China. Inverse modeling estimates by *Pétron et al.* [2004], using MOPITT measurements to estimate emissions, concluded that emissions for the USA and eastern Asia had been higher than original model emission estimates for those regions. Those regions had predominantly non-biomass-burning emissions based on Emission Database for Global Atmospheric Research, version 3 (EDGAR-3) emission estimates [*Olivier and Berdowski*, 2001]. These estimates are also used in the TM4 model, which thus may explain the lower modeled CO columns over the USA and eastern Asia.

[48] Figure 9 shows the spatial distribution of the average of the absolute differences between measured and modeled monthly mean CO total columns for the period September 2003 to August 2004. This is a simple test to investigate the agreement between modeled and measured seasonal cycles. The TM4 model results indicate that the dominant CO total column variability occurs on monthly timescales, so comparing modeled and measured seasonal cycles (monthly means) is an important test of the quality of monthly averaged SCIAMACHY CO total column measurements. Comparing Figure 9 with Figure 7 shows that differences between measured and modeled seasonal cycles are generally smaller for measurements with smaller instrument noise errors. Occasionally large differences in combination with small noise errors do occur, most notably over southern

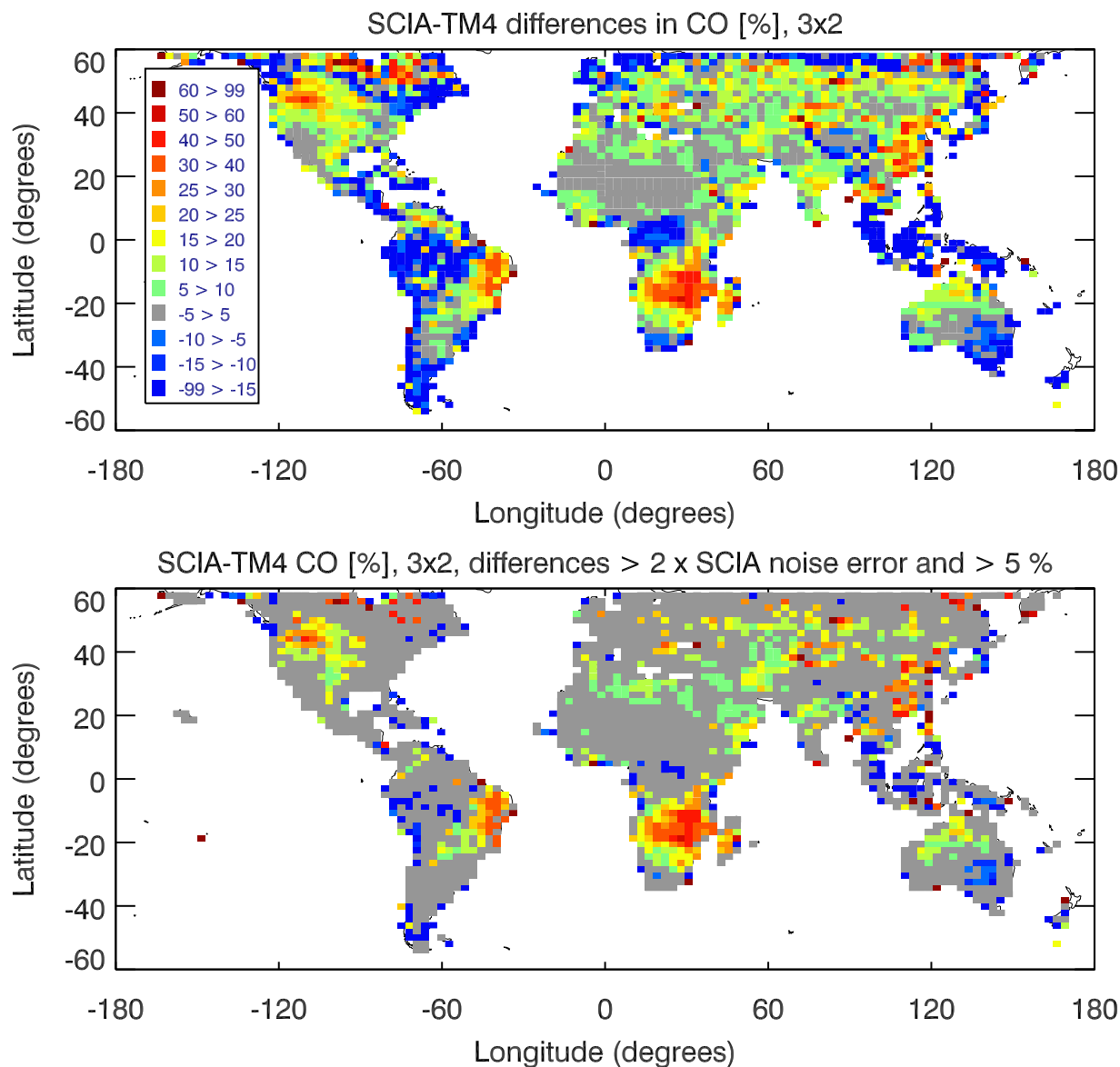


Figure 8. (top) Differences between SCIAMACHY and TM4 CO total column measurement as percentage of the TM4 CO total column measurements for the period September 2003 to August 2004 for the same selection of grids as shown in Figure 6. The grey pixels indicate locations with instrument noise errors smaller than 5%. (bottom) Similar to Figure 8 (top) but only differences that are larger than the $2\text{-}\sigma$ instrument noise errors and larger than 5% of the modeled total CO column are shown. All other pixels are shown in grey.

Africa, which was also noted by *Gloudemans et al.* [2006], and likely related to inaccurate model emissions.

[49] Figure 10 compares the results in Figures 7 and 9 by showing a scatterplot of the average of the absolute monthly differences versus instrument noise errors. The grey line indicates the $2\text{-}\sigma$ noise error (95% confidence level). A linear relation is found between the differences and instrument noise errors with a correlation coefficient of 0.85. For small noise errors ($<0.03 \times 10^{18}$ molecules/cm²) most differences are significant while for larger errors more differences are not significant. Figure 10 also shows that for instrument noise errors smaller than 0.05×10^{18} molecules/cm² the average of the absolute monthly differences between modeled and measured CO total columns are

not smaller than $0.05\text{--}0.1 \times 10^{18}$ molecules/cm². This is an indication that errors other than instrument noise errors, like those described in section 2, also contribute to measurement-model differences. However, these errors are relatively small compared to the typical seasonal cycles of CO total columns as can be seen in Figure 3 where the typical amplitude in the seasonality of monthly mean CO total columns ranges from 0.2 to 1×10^{18} molecules/cm².

5. Summary and Conclusions

[50] This paper presents a detailed systematic and quantitative cross evaluation of SCIAMACHY CO total column measurements and CTM model results.

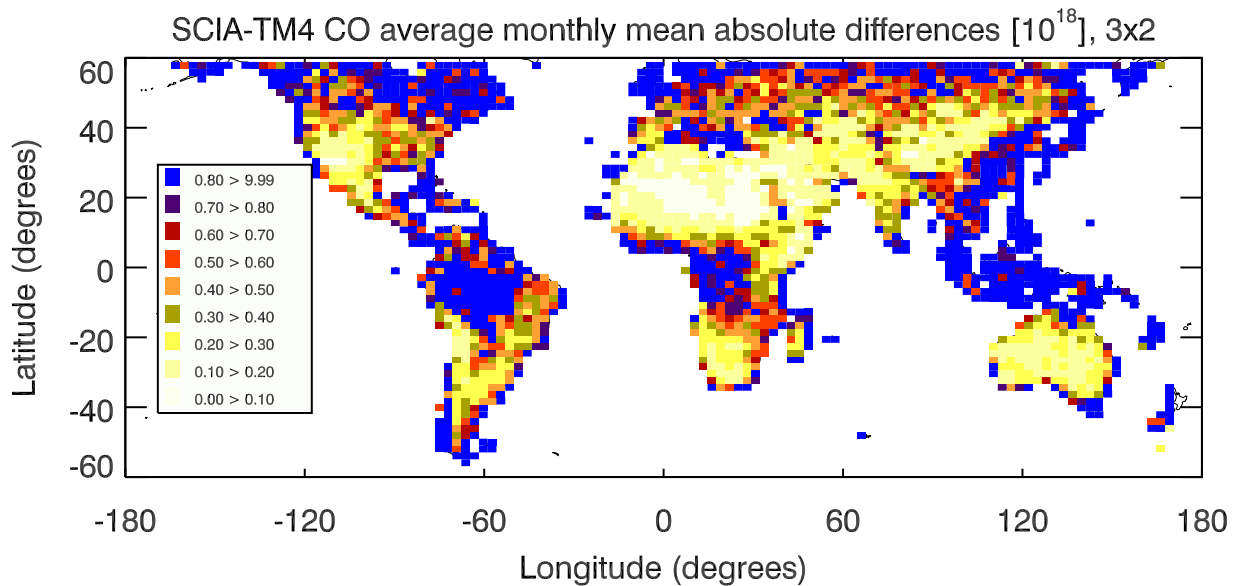


Figure 9. Average absolute monthly mean differences between SCIAMACHY and TM4 CO total columns as fraction of the corresponding annual mean TM4 CO total columns for the period September 2003 to August 2004 and the same selection of grids as shown in Figure 6.

[51] Annual and monthly mean measured and modeled CO total column measurements are compared with modeled CO total columns using results from two TM4 model simulations with either climatological CO BB-emissions or GFEDv2 CO BB-emissions based on actual remote sensing data. A much better agreement between modeled and measured CO total columns is found for the model simulation with GFEDv2 BB-emissions compared to climatological BB-emissions. Many remaining differences are not statistically significant at the 95% confidence level (2σ

instrument noise error). Some significant differences remain, particularly over regions in northwestern USA, eastern South America, southern Africa and eastern China. These are typically regions of high and variable CO sources (biomass burning, growing industrial activity), and it shows the potential of SCIAMACHY measurements to improve CO emission databases.

[52] A statistical analysis based on single measurements and temporally and spatially collocated model results shows that they agree quite well within measurement uncertainties.

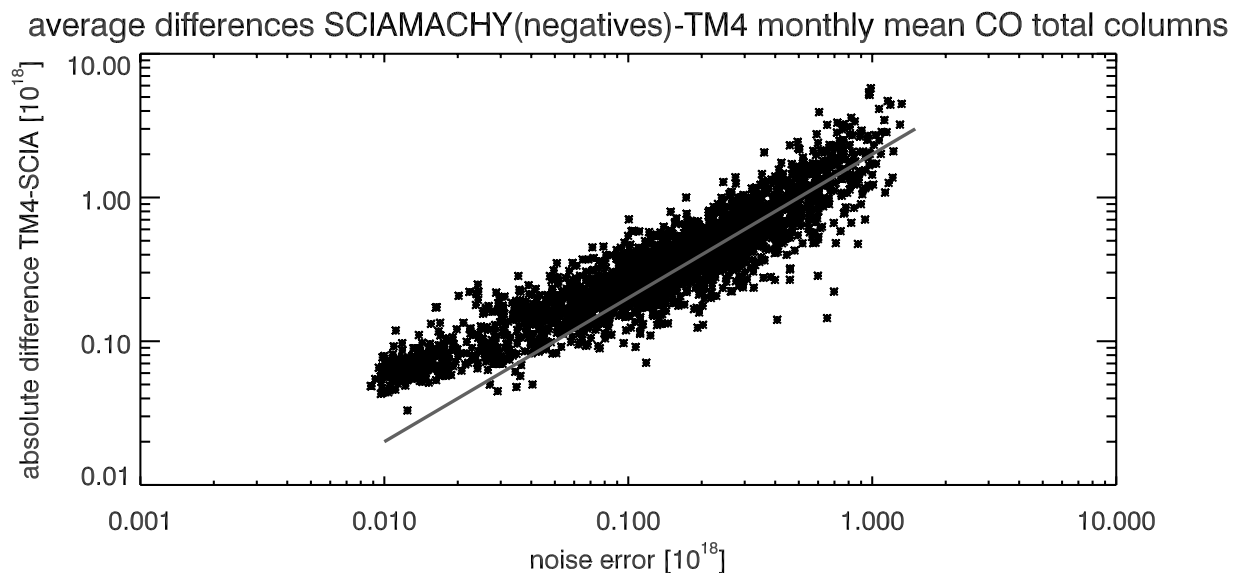


Figure 10. Scatterplot of the average monthly mean instrument noise errors shown in Figure 7 versus the average absolute differences in monthly mean SCIAMACHY and TM4 CO total columns shown in Figure 9 for the period September 2003 to August 2004. The grey line indicates two times the instrument noise error level. Differences to the left of this line are considered statistically significant at the 95% confidence level.

Differences between measured and modeled CO total columns are dominated by the instrument noise error. For very large instrument noise errors ($>1-2 \times 10^{18}$ molecules/cm²) the measurements are positively biased and these measurements (instrument noise error $>1.5 \times 10^{18}$ molecules/cm²) are currently excluded from the calculation of annual and monthly means. Measured CO total columns can become negative in case of instrument noise errors $>0.2 \times 10^{18}$ molecules/cm². Such measurements should not be excluded from the analysis because this can result in positive measurement biases when averaging data with large instrument noise errors. All negative CO columns have therefore been included in our analysis, given that their instrument noise error was smaller than 1.5×10^{18} molecules/cm².

[53] The instrument noise errors of SCIAMACHY CO total column measurements are closely related to surface albedo and the number of SCIAMACHY measurements within a region and time period that are averaged. The spatial distributions of surface albedo and cloud cover are very similar, i.e., high surface albedos (>0.2) occur over arid and semiarid regions (deserts), which are also regions with low cloud cover. These distributions reinforce each other which results in large spatial variations of instrument noise errors in monthly and annual mean SCIAMACHY CO total column measurements. Regions with an albedo >0.2 and more than 80% cloud free scenes have instrument noise errors for monthly or annual means that can be up to 25 times smaller than instrument noise errors for low albedo/high cloud cover regions, i.e., albedo <0.1 and $<20\%$ cloud free scenes.

[54] The spatial distribution of average absolute differences between monthly mean measurements and model results is very similar to the spatial distribution of instrument noise errors: differences are smaller at locations with smaller errors (Figures 7, 9, and 10). The agreement between measurements and model results indicates that overall no large biases are present. A few occasions are found in which the monthly mean SCIAMACHY columns are significantly smaller than the modeled CO columns (Figure 3). These differences are likely related to cloud cover within a SCIAMACHY pixel over low surface albedo locations. For such a situation most of the information on CO comes from the clouded scene because of the relatively high reflectance of clouds in the near-infrared, despite the low cloud cover.

[55] The comparison of differences between SCIAMACHY and TM4 and their statistical analysis both indicate that other error sources, such as systematic retrieval errors, spectroscopic errors, aerosols and model errors, are about $0.05-0.1 \times 10^{18}$ molecules/cm², which is in line with independent estimates of these errors. This indicates that currently our best estimate of the achievable accuracy of SCIAMACHY monthly mean CO total columns is $0.05-0.1 \times 10^{18}$ molecules/cm².

[56] Monthly averaged SCIAMACHY CO total columns have sufficiently small instrument noise errors for studying seasonal variations of CO total columns. These measurements are likely good enough to improve on modeling errors due to uncertainties in emission inventories. However, total column measurements at locations with surface albedos <0.1 are often too noisy to contain useful information on CO total column seasonal variations. The

SCIAMACHY CO total columns provide measurements with a unique sensitivity to the lower troposphere and thus complement existing tropospheric CO measurements by for example MOPITT.

[57] **Acknowledgments.** SCIAMACHY is a joint project of the German Space Agency DLR and the Dutch Space Agency NIVR with contribution of the Belgian Space Agency BUSOC. The authors thank the Netherlands SCIAMACHY Data Center and ESA for providing data. The authors specifically thank Sander Houweling for kindly providing CTM modeled CH₄ fields that have been used for the empirical correction for the SCIAMACHY channel 8 ice layer and Otto Hasekamp for providing estimates of the retrieval uncertainty due to aerosols. This work is partly financed by the European Commission (5th Framework Programme, project EVERGREEN) and NIVR.

References

- Arellano, A. F., Jr., P. S. Kasibhatla, L. Giglio, G. R. van der Werf, J. T. Randerson, and G. J. Collatz (2006), Time-dependent inversion estimates of global biomass-burning CO emissions using Measurement of Pollution in the Troposphere (MOPITT) measurements, *J. Geophys. Res.*, *111*, D09303, doi:10.1029/2005JD006613.
- Barret, B., M. De Mazière, and E. Mahieu (2003), Ground-based FTIR measurements of CO from the Jungfraujoch: Characterization and comparison with in situ surface and MOPITT data, *Atmos. Chem. Phys.*, *3*, 2217–2223.
- Bregman, B., et al. (2003), On the use of mass-conserving wind fields in chemistry–Transport models, *Atmos. Chem. Phys.*, *3*, 447–457.
- Bremer, H., et al. (2004), Spatial and temporal variation of MOPITT CO in Africa and South America: A comparison with SHADOZ ozone and MODIS aerosol, *J. Geophys. Res.*, *109*, D12304, doi:10.1029/2003JD004234.
- Buchwitz, M., et al. (2004), Global carbon monoxide as retrieved from SCIAMACHY by WFM-DOAS, *Atmos. Chem. Phys.*, *4*, 1945–1960.
- Buchwitz, M., et al. (2005), Carbon monoxide, methane and carbon dioxide columns retrieved from SCIAMACHY by WFM-DOAS: Year 2003 initial data set, *Atmos. Chem. Phys.*, *5*, 3313–3329.
- Buchwitz, M., et al. (2006), Atmospheric carbon gases retrieved from SCIAMACHY by WFM-DOAS: Version 0.5, CO and CH₄ and impact of calibration improvements on CO₂ retrieval, *Atmos. Chem. Phys.*, *6*, 2727–2751.
- Crawford, J. H., et al. (2004), Relationship between Measurements of Pollution in the Troposphere (MOPITT) and in situ observations of CO based on a large-scale feature sampled during TRACE-P, *J. Geophys. Res.*, *109*, D15S04, doi:10.1029/2003JD004308.
- Deeter, M. N., et al. (2003), Operational carbon monoxide retrieval algorithm and selected results for the MOPITT instrument, *J. Geophys. Res.*, *108*(D14), 4399, doi:10.1029/2002JD003186.
- Deeter, M. N., et al. (2004a), Evaluation of operational radiances for the Measurements of Pollution in the Troposphere (MOPITT) instrument CO thermal band channels, *J. Geophys. Res.*, *109*, D03308, doi:10.1029/2003JD003970.
- Deeter, M. N., L. K. Emmons, D. P. Edwards, J. C. Gille, and J. R. Drummond (2004b), Vertical resolution and information content of CO profiles retrieved by MOPITT, *Geophys. Res. Lett.*, *31*, L15112, doi:10.1029/2004GL020235.
- de Laat, A. T. J., A. M. S. Gloudemans, H. Schrijver, M. M. P. van den Broek, J. F. Meirink, I. Aben, and M. Krol (2006), Quantitative analysis of SCIAMACHY carbon monoxide total column measurements, *Geophys. Res. Lett.*, *33*, L07807, doi:10.1029/2005GL025530.
- Dentener, F., et al. (2003), Trends and inter-annual variability of methane emissions derived from 1979–1993 global CTM simulations, *Atmos. Chem. Phys.*, *3*, 73–88.
- Dils, B., et al. (2006), Comparisons between SCIAMACHY and ground-based FTIR data for total columns of CO, CH₄, CO₂ and N₂O, *Atmos. Chem. Phys.*, *6*, 1953–1976.
- Edwards, D. P., et al. (2004), Observations of carbon monoxide and aerosols from the Terra satellite: Northern Hemisphere variability, *J. Geophys. Res.*, *109*, D24202, doi:10.1029/2004JD004727.
- Edwards, D. P., et al. (2006), Satellite-observed pollution from Southern Hemisphere biomass burning, *J. Geophys. Res.*, *111*, D14312, doi:10.1029/2005JD006655.
- Emmons, L. K., et al. (2004), Validation of Measurements of Pollution in the Troposphere (MOPITT) CO retrievals with aircraft in situ profiles, *J. Geophys. Res.*, *109*, D03309, doi:10.1029/2003JD004101.
- Frankenberg, C., U. Platt, and T. Wagner (2005), Retrieval of CO from SCIAMACHY onboard ENVISAT: Detection of strongly polluted areas

- and seasonal patterns in global CO abundances, *Atmos. Chem. Phys.*, *5*, 1639–1644.
- Galanter, M., H. Levy II, and G. R. Carmichael (2000), Impacts of biomass burning on tropospheric CO, NO_x and O₃, *J. Geophys. Res.*, *105*, 6633–6653.
- Gloude-mans, A. M. S., et al. (2005), The impact of SCIAMACHY near-infrared instrument calibration on CH₄ and CO total columns, *Atmos. Chem. Phys.*, *5*, 2369–2383.
- Gloude-mans, A. M. S., M. C. Krol, J. F. Meirink, A. T. J. de Laat, G. R. van der Werf, H. Schrijver, M. M. P. van den Broek, and I. Aben (2006), Evidence for long-range transport of carbon monoxide in the Southern Hemisphere from SCIAMACHY observations, *Geophys. Res. Lett.*, *33*, L16807, doi:10.1029/2006GL026804.
- Granier, C., W. M. Hao, G. Brasseur, and J.-D. Müller (1996), Land-use practice and biomass burning: Impacts on the chemical composition of the atmosphere, in *Biomass Burning and Global Change*, edited by J. S. Levine, pp 140–198, MIT Press, Cambridge, Mass.
- Granier, C., G. Pétron, J.-F. Müller, and G. Brasseur (2000), The impact of natural and anthropogenic hydrocarbons on the tropospheric budget of carbon monoxide, *Atmos. Environ.*, *24*, 5255–5270.
- Hao, W. M., and M. H. Liu (1994), Spatial and temporal distribution of tropical biomass burning, *Global Biogeochem. Cycles*, *8*, 495–503.
- Heald, C. L., et al. (2003), Asian outflow and trans-Pacific transport of carbon monoxide and ozone pollution: An integrated satellite, aircraft, and model perspective, *J. Geophys. Res.*, *108*(D24), 4804, doi:10.1029/2003JD003507.
- Holloway, T., H. Levy II, and P. Kasibhatla (2000), Global distribution of carbon monoxide, *J. Geophys. Res.*, *105*(D10), 12,123–12,148.
- Houweling, S., F. J. Dentener, and J. Lelieveld (1998), The impact of non-methane hydrocarbon compounds on tropospheric photochemistry, *J. Geophys. Res.*, *103*, 10,673–10,696.
- Kleipool, Q. L., et al. (2007), In-flight proton-induced radiation damage to SCIAMACHY's extended-wavelength InGaAs near-infrared detectors, *Infrared Phys. Technol.*, *50*, 30–37.
- Krijger, J. M., I. Aben, and H. Schrijver (2005), Distinction between clouds and ice/snow covered surfaces in the identification of cloud-free observations using SCIAMACHY PMDs, *Atmos. Chem. Phys.*, *5*, 2729–2738.
- Lamarque, J.-F., et al. (2003), Identification of CO plumes from MOPITT data: Application to the August 2000 Idaho-Montana forest fires, *Geophys. Res. Lett.*, *30*(13), 1688, doi:10.1029/2003GL017503.
- Langenfelds, R. L., R. J. Francey, B. C. Pak, L. P. Steele, J. Lloyd, C. M. Trudinger, and C. E. Allison (2002), Interannual growth rate variations of atmospheric CO₂ and its δ¹³C, H₂, CH₄, and CO between 1992 and 1999 linked to biomass burning, *Global Biogeochem. Cycles*, *16*(3), 1048, doi:10.1029/2001GB001466.
- Lee, S., G.-H. Choi, H.-S. Lim, and J.-H. Lee (2004), Global and regional distribution of carbon monoxide from MOPITT: seasonal distribution at 700 hPa, *Environ. Monit. Assess.*, *92*, 35–42.
- Lelieveld, J., F. J. Dentener, W. Peters, and M. C. Krol (2004), On the role of hydroxyl radicals in the self-cleansing capacity of the troposphere, *Atmos. Chem. Phys.*, *4*, 2337–2344.
- Lichtenberg, G., et al. (2006), SCIAMACHY Level 1 data: Calibration concept and in-flight calibration, *Atmos. Chem. Phys.*, *6*, 5347–5367.
- McMillan, W. W., C. Barnet, L. Strow, M. T. Chahine, M. L. McCourt, J. X. Warner, P. C. Novelli, S. Korontzi, E. S. Maddy, and S. Datta (2005), Daily global maps of carbon monoxide from NASA's Atmospheric Infrared Sounder, *Geophys. Res. Lett.*, *32*, L11801, doi:10.1029/2004GL021821.
- Meirink, J. F., H. J. Eskes, and A. P. H. Goede (2006), Sensitivity analysis of methane emissions derived from SCIAMACHY observations through inverse modeling, *Atmos. Chem. Phys.*, *6*, 1275–1292.
- Novelli, P. C., K. A. Masarie, P. M. Lang, B. D. Hall, R. C. Myers, and J. W. Elkins (2003), Reanalysis of tropospheric CO trends: Effects of the 1997–1998 wildfires, *J. Geophys. Res.*, *108*(D15), 4464, doi:10.1029/2002JD003031.
- Olivier, J. G. J., and J. J. M. Berdowski (2001), Global emission sources and sinks, in *The Climate System*, edited by J. Berdowski et al., pp. 33–78, Balkema, A. A., Brookfield, Vt.
- Pétron, G., C. Granier, B. Khattatov, J. Lamarque, V. Yudin, J. Müller, and J. Gille (2002), Inverse modeling of carbon monoxide surface emissions using Climate Monitoring and Diagnostics Laboratory network observations, *J. Geophys. Res.*, *107*(D24), 4761, doi:10.1029/2001JD001305.
- Pétron, G., C. Granier, B. Khattatov, V. Yudin, J.-F. Lamarque, L. Emmons, J. Gille, and D. P. Edwards (2004), Monthly CO surface sources inventory based on the 2000–2001 MOPITT satellite data, *Geophys. Res. Lett.*, *31*, L21107, doi:10.1029/2004GL020560.
- Pfister, G., G. Pétron, L. K. Emmons, J. C. Gille, D. P. Edwards, J.-F. Lamarque, J.-L. Attie, C. Granier, and P. C. Novelli (2004), Evaluation of CO simulations and the analysis of the CO budget for Europe, *J. Geophys. Res.*, *109*, D19304, doi:10.1029/2004JD004691.
- Rodgers, C. D., and B. J. Connor (2003), Intercomparison of remote sounding instruments, *J. Geophys. Res.*, *108*(D3), 4116, doi:10.1029/2002JD002299.
- Shindell, D. T., et al. (2006), Multimodel simulations of carbon monoxide: Comparison with observations and projected near-future changes, *J. Geophys. Res.*, *111*, D19306, doi:10.1029/2006JD007100.
- Sussmann, R., and M. Buchwitz (2005), Initial validation of ENVISAT/SCIAMACHY columnar CO by FTIR profile retrievals at the Ground-Truthing Station Zugspitze, *Atmos. Chem. Phys.*, *5*, 1497–1503.
- Taylor, K. E. (2001), Summarizing multiple aspects of model performance in a single diagram, *J. Geophys. Res.*, *106*(D7), 7183–7192.
- van Aardenne, J. A., F. J. Dentener, J. G. J. Olivier, C. G. M. Klein Goldewijk, and J. Lelieveld (2001), A 1° × 1° resolution data set of historical anthropogenic trace gas emissions for the period 1890–1990, *Global Biogeochem. Cycles*, *15*(4), 909–928.
- van der Werf, J., et al. (2006), Interannual variability in global biomass burning emissions from 1997 to 2004, *Atmos. Chem. Phys.*, *6*, 3423–3441.
- Velazco, V., J. Notholt, T. Warneke, M. Lawrence, H. Bremer, J. Drummond, A. Schulz, J. Krieg, and O. Schrems (2005), Latitude and altitude variability of carbon monoxide in the Atlantic detected from ship-borne Fourier transform spectrometry, model, and satellite data, *J. Geophys. Res.*, *110*, D09306, doi:10.1029/2004JD005351.
- Wotawa, G., P. C. Novelli, M. Trainer, and C. Granier (2001), Inter-annual variability of summertime CO concentrations in the Northern Hemisphere explained by boreal forest fires in North America and Russia, *Geophys. Res. Lett.*, *28*(24), 4575–4578.
- Yudin, V. A., G. Pétron, J.-F. Lamarque, B. V. Khattatov, P. G. Hess, L. V. Lyjak, J. C. Gille, D. P. Edwards, M. N. Deeter, and L. K. Emmons (2004), Assimilation of the 2000–2001 CO MOPITT retrievals with optimized surface emissions, *Geophys. Res. Lett.*, *31*, L20105, doi:10.1029/2004GL021037.
- Yurganov, L. (2000), Carbon monoxide inter-annual variations and trends in the Northern Hemisphere: Role of OH, *Int. Global Atmos. Chem. NewsL.*, *21*. (Available at <http://www.igac.noaa.gov/newsletter/21/trends.php>)
- Yurganov, L. N., et al. (2005), Increased Northern Hemispheric carbon monoxide burden in the troposphere in 2002 and 2003 detected from ground and from space, *Atmos. Chem. Phys.*, *5*, 563–573.

I. Aben, A. M. S. Gloude-mans, M. Krol, and H. Schrijver, SRON, Sorbonnelaan 2, NL-3584 CA Utrecht, Netherlands.

A. T. J. de Laat, KNMI, Wilhelminalaan 10, NL-3732 GK de Bilt, Netherlands. (jos.de.laat@knmi.nl)

J. F. Meirink, IMAU, Utrecht University, P.O. Box 80005, NL-3508 TA Utrecht, Netherlands.

G. R. van der Werf, Faculty of Earth and Life Sciences, Free University, De Boelelaan NL-1085, 1081 HV Amsterdam, Netherlands.